Effect of host glass on the optical absorption properties of Nd^{3+}, Sm^{3+}, and Dy^{3+} in lead borate glasses

M. B. Saisudha and J. Ramakrishna
Department of Physics, Indian Institute of Science, Bangalore 560012, India
(Received 27 June 1995; revised manuscript received 10 November 1995)

The effect of host glass composition on the optical absorption spectra of Nd^{3+}, Sm^{3+}, and Dy^{3+} in lead borate glasses, with PbO contents varying from 30 to 70 mol %, has been analyzed using Judd-Ofelt theory and the compositional dependence has been determined for the hypersensitive bands. Judd-Ofelt intensity parameters Ω_t ($t=2,4,6$), and the radiative transition probabilities. The variation of Ω_2 with PbO content has been attributed to changes in the asymmetry of the ligand field at the rare-earth (R) site (due to the structural changes) and to changes in R-O covalency, whereas the variation of Ω_6 has been related to the variation in R-O covalency. The radiative transition probabilities of the rare-earth ions are large in lead borate glasses suggesting their suitability for laser applications.

I. INTRODUCTION

The increasing importance of glasses doped with rare-earth ions as possible lasing materials has created considerable interest in the study of optical-absorption and fluorescence properties of rare-earth ions in glasses. Glasses are promising hosts[1] to investigate the influence of chemical environment on the optical properties of the rare earth ions. The extensive investigations of absorption and luminescent properties of the Nd^{3+},[2–7] Sm^{3+},[8–11] and Dy^{3+},[12] ions have indicated that the optical properties of these rare-earth ions can be affected by varying the glass composition.

The Judd-Ofelt theory[13,14] has been successfully used in estimating the intensities of the transitions for rare-earth ions. This theory defines a set of three intensity parameters Ω_t ($t=2,4,6$) that are sensitive to the environment of the rare-earth ion. From these parameters, important optical properties such as the radiative transition probability for spontaneous emission, radiative lifetime of the excited states, and branching ratios (which predict the fluorescence intensity of laser transitions) can be estimated and used further to examine the dependence of the spectroscopic parameters on the glass composition. In order to increase the laser efficiency of a particular transition, the stimulated emission cross section should be made as large as possible. It is therefore important to optimize the relation between the glass composition and the Ω_t parameters and the radiative transition probability (which determines the stimulated emission cross section) to yield favorable spectroscopic properties for a given laser application.

In the present work, the effect of a lead borate matrix on the optical properties of Nd^{3+}, Sm^{3+}, and Dy^{3+} ions is investigated. Lead borate glasses have a large glass-forming range ($\approx$25–80 mol % PbO), a high refractive index (1.6–2.0), and a strong absorption in the ultraviolet region[15] and are thus interesting systems in which to study the effect of host composition on the optical properties of rare-earth ions. Structural groups like boroxol, pentaborates, and diborates containing three and four coordinated borons, and ring- and chain-type metaborate groups containing nonbridging oxygens, are found to be present in lead borate glasses[16,17] for different PbO concentrations, and it would be interesting to study the correlation between these structural groups and the intensity parameters. The structural groups present in lead borate glasses are shown in Fig. 1.

II. THE JUDD-OFELT THEORY

The absorption spectra of rare-earth ions serve as a basis for understanding their radiative properties. The sharp absorption lines arising from the $4f$-$4f$ electronic transitions can be electric dipole, magnetic dipole, or electric quadrupole in character. The quantitative calculation of the intensities of these transitions has been developed independently by

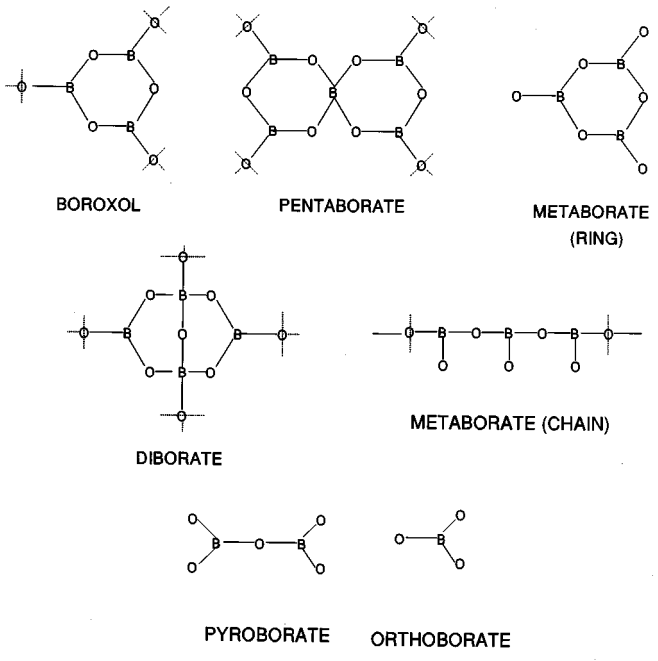

FIG. 1. Various structural groups present in $(100\text{-}x)B_2O_3$:xPbO glasses (Ref. 17).

Judd[13] and by Ofelt.[14] A brief outline of the Judd-Ofelt theory is given below.

For a free rare-earth ion the electric dipole transitions between two states within the $4f$ configuration are parity forbidden, while the magnetic dipole and electric quadrupole transitions are allowed. For an ion in a medium, the electric dipole transitions become allowed because of the admixture of states from configurations of opposite parity (for example, $4f^{N-1}5d$) into the $4f$ configuration. The transition probability depends on the extent of admixture.

A. The oscillator strength

The intensity of an absorption band is expressed in terms of a quantity called the ''oscillator strength.'' Experimentally, it is given by the area under the absorption band. The oscillator strength f_{meas} can be expressed in terms of the absorption coefficient $\alpha(\lambda)$ at a particular wavelength λ and is given by[18]

$$f_{\text{meas}}=\frac{mc^2}{\pi e^2 N}\int \frac{\alpha(\lambda)d\lambda}{\lambda^2}, \tag{1}$$

where $\alpha(\lambda)=(2.303)D_O(\lambda)/d$ is the measured absorption coefficient at a given wavelength λ. $D_O(\lambda)$ is the optical density $[\log_{10}(I/I_0)]$ as a function of wavelength λ, d the thickness of the sample in cm, m and e are the mass and charge of the electron respectively, c is the velocity of light, and N is the number of rare-earth ions per unit volume. The absorption bands in glasses are broad because of the disorder and are generally not pure Gaussians. It is usually a good approximation to use a Gaussian error curve[19]

$$\epsilon=\epsilon_{\max}2^{-(\nu-\nu_o)^2/\Delta\nu_{1/2}^2}, \tag{2}$$

where $\epsilon_{\max}=D_O(\nu)/dN$.

Here, ν_o is the frequency of the absorption band at which the molar extinction coefficient ϵ is maximum. $\Delta\nu_{1/2}$ is the half bandwidth (in cm^{-1}). Then the expression for oscillator strength Eq. (1) can be written in energy units (in cm^{-1}) as

$$f_{\text{meas}}=2.303\,\frac{mc^2}{\pi e^2 N}\,2.1289\epsilon_{\max}\Delta\nu_{1/2}. \tag{3}$$

According to the Judd-Ofelt theory[20] the oscillator strength of a transition between an initial J manifold $(S,L)J$ and a final J manifold $(S',L')J'$ is given by

$$f_{\text{cal}}(aJ,bJ')=\frac{8\pi^2 m\nu}{3h(2J+1)}\left[\frac{(n^2+2)^2}{9n}S_{\text{ed}}+nS_{\text{md}}\right], \tag{4}$$

where

$$S_{\text{ed}}[(S,L)J;(S',L')J']$$

$$=\sum_{t=2,4,6}\Omega_t|\langle(S,L)J\|U^{(t)}\|(S',L')J'\rangle|^2 \tag{5}$$

and

$$S_{\text{md}}[(S,L)J;(S',L')J']$$

$$=\sum_{t=2,4,6}\Omega_t|\langle(S,L)J\|L+2S\|(S',L')J'\rangle|^2, \tag{6}$$

where S_{ed} and S_{md} represent the line strengths for the induced electric dipole transition and the magnetic dipole transition, respectively.

The three intensity parameters Ω_t $(t=2,4,6)$ are characteristic of a given rare-earth ion (in a given matrix) and are related to the radial wave functions of the states $4f^N$ and the admixing states $4f^{N-1}5d$ or $4f^{N-1}5g$ and the ligand field parameters that characterize the environmental field. They are given by the expression,

$$\Omega_t=(2t+1)\sum_{s,p}|A_{s,p}|^2\Xi^2(s,t)(2s+1)^{-1}, \quad t=2,4,6, \tag{7}$$

where $A_{s,p}$ are the crystal-field parameters of rank s and are related to the structure around the rare-earth ions. $\Xi(s,t)$ is related to the matrix elements between the two radial wave functions of $4f$ and the admixing levels, e.g., $5d$, $5g$, and the energy difference between these two levels. It has been suggested by Reisfeld[21] that Ξ correlates to the nephlauxetic parameter β, which indicates the degree of covalency of the R—O bond by[22]

$$\Xi(s,t)\propto\beta=\frac{\nu_f-\nu}{\nu_f}, \tag{8}$$

where ν_f and ν are the transition energy of the free ion and the ion in a glass, respectively.

$|\langle\|U^{(t)}\|\rangle|^2$ represents the square of the matrix elements of the unit tensor operators $U^{(t)}$ connecting the initial and final states. The matrix elements are calculated in the intermediate coupling approximation.[23] Because of the electrostatic shielding of the $4f$ electrons by the closed $5p$ shell electrons, the matrix elements of the unit tensor operator between two energy manifolds in a given rare-earth ion do not vary significantly when it is incorporated in different hosts. Therefore, the matrix elements computed for the free ion may be used for further calculations in different media and are reported by Weber[24] and Carnall, Fields, and Rajnak.[25] The reduced matrix elements $\langle\|L+2S\|\rangle$ for magnetic dipole transitions are reported by Neilson and Koster.[26]

The line strengths for both electric and magnetic dipole transitions are related to the integrated absorption coefficient and are given by[27]

$$\int_{\text{band}}K(\lambda)d\lambda=\frac{8\pi^3\lambda N}{3ch(2J+1)n^2}[\chi_{\text{ed}}S_{\text{ed}}+\chi_{\text{md}}S_{\text{md}}], \tag{9}$$

where $\chi_{\text{ed}}=n(n^2+2)^2/9$ and $\chi_{\text{md}}=n^3$ are the terms that correct the effective field at a well-localized center in a medium of isotropic refractive index n. $K(\lambda)$ is the absorption coefficient at mean wavelength λ, N is the concentration of the rare-earth ions, c is the velocity of light, h is Planck's constant, e is the electronic charge, and J is the total angular momentum of the initial state. Using the values of the integrated absorption coefficient, the oscillator strength f_{cal} of various bands can be calculated using the expression

$$f_{\text{cal}}=\frac{mc^2}{N\pi\lambda^2}\int K(\lambda)d\lambda \quad \text{or} \quad f_{\text{cal}}=\frac{mc^2}{N\pi}\int K(\nu)d\nu, \tag{10}$$

where m is the mass of the electron.

B. Radiative transition probability for induced electric dipole emission

The Ω_t values thus obtained from the absorption measurements are further used to calculate the radiative transition probability, radiative lifetime of the excited states and branching ratios (which predict the fluorescence intensity of the lasing transition). The radiative transition probability $A_{\text{rad}}(aJ,bJ')$ for emission from an initial state aJ to a final ground state bJ' is given by[28]

$$A_{\text{rad}}(aJ,bJ')=\frac{64\pi^4\nu^3e^2}{3hc^3(2J+1)}\left[\frac{n(n^2+2)^2}{9}S_{\text{ed}}+n^3S_{\text{md}}\right]. \tag{11}$$

In the case of electric dipole emission, this equation becomes

$$A_{\text{rad}}(aJ,bJ')=\frac{64\pi^4\nu^3}{3hc^3(2J+1)}\frac{n(n^2+2)^2}{9}e^2 \times\sum_{t=2,4,6}\Omega_t|\langle(S,L)J\|U^{(t)}\|(S',L')J'\rangle|^2. \tag{12}$$

The total radiative emission probability $A_T(aJ)$ of the $S'L'J'$ excited state [$^4F_{3/2}(Nd^{3+})$, $^4G_{5/2}(Sm^{3+})$, and $^6H_{15/2}(Dy^{3+})$] is given by the sum of the $A_{\text{rad}}(aJ,bJ')$ terms calculated over all terminal states b

$$A_T(aJ)=\sum_{bJ'}A_{\text{rad}}(aJ,bJ'). \tag{13}$$

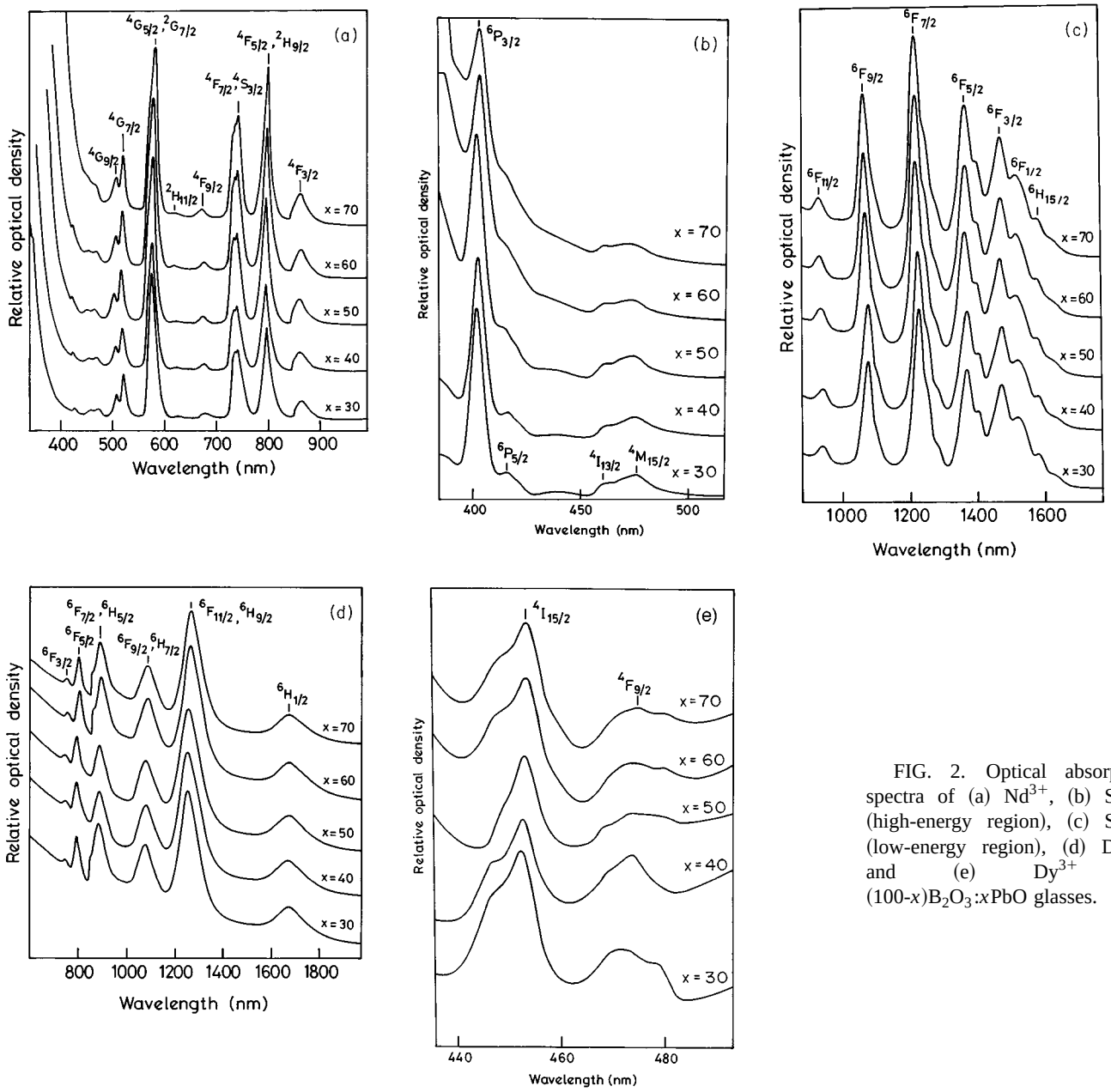

FIG. 2. Optical absorption spectra of (a) Nd^{3+}, (b) Sm^{3+} (high-energy region), (c) Sm^{3+} (low-energy region), (d) Dy^{3+}, and (e) Dy^{3+} in $(100\text{-}x)B_2O_3$:xPbO glasses.

TABLE I. Oscillator strengths, refractive index, density, and Judd-Ofelt parameters of Nd^{3+} (3 mol %) in (100-x) B_2O_3:xPbO glasses.

Transitions from the ground state $^4I_{9/2}$	λ (nm)	Oscillator strength ($f\times10^{-8}$)									
		BPN30		BPN40		BPN50		BPN60		BPN70	
		f_{meas}	f_{cal}	f_{meas}	f_{cal}	f_{meas}	f_{cal}	f_{meas}	f_{cal}	f_{meas}	f_{cal}
$^4F_{3/2}$	866	213.6	214.5	215.2	217.1	200.2	202.2	205.5	210.4	225.7	230.9
$^4F_{5/2},^2H_{9/2}$	801	576.3	580.9	625.3	628.7	625.2	627.9	654.7	654.0	726.0	731.2
$^4F_{7/2},^4S_{3/2}$	745	495.2	492.5	553.8	551.7	571.5	569.9	593.6	593.9	672.4	669.2
$^4F_{9/2}$	679	60.4	58.5	62.5	64.7	64.9	66.2	66.6	68.9	73.6	77.3
$^4G_{5/2},^4G_{7/2}$ (HST)	581	1488	1488	1435	1435	1421	1421	1486	1485	1598	1598
$^4K_{13/2},^4G_{9/2},^4G_{7/2}$	524	484.2	480.4	493.1	489.4	473.9	470.6	494.9	490.2	546.0	538.4
$^2G_{9/2},^4G_{11/2},^2D_{3/2}$	473	46.3	44.3	49.4	46.9	48.1	46.1	50.1	48.1	54.1	53.5
RMS deviation		0.410%		0.570%		0.319%		0.400%		0.592%	
Density (g/cm^3)		4.232 ± 0.024		4.589 ± 0.029		5.068 ± 0.026		5.519 ± 0.032		6.032 ± 0.032	
N (10^{20} cm^{-3})		12.10 ± 0.068		11.75 ± 0.076		11.71 ± 0.061		11.61 ± 0.067		11.66 ± 0.051	
Refractive index		1.660 ± 0.01		1.723 ± 0.01		1.762 ± 0.01		1.812 ± 0.01		1.916 ± 0.01	
$\Omega_2\times10^{-20}$ cm^2		3.958 ± 0.067		3.588 ± 0.110		3.590 ± 0.222		3.613 ± 0.235		3.523 ± 0.227	
$\Omega_4\times10^{-20}$ cm^2		3.773 ± 0.009		3.501 ± 0.033		3.024 ± 0.125		3.029 ± 0.141		2.984 ± 0.062	
$\Omega_6\times10^{-20}$ cm^2		4.882 ± 0.079		5.262 ± 0.160		5.320 ± 0.160		5.329 ± 0.284		5.480 ± 0.225	

The fluorescence branching ratio β_R is given as

$$\beta_R=\frac{A(aJ,bJ')}{A_T(aJ)}. \tag{14}$$

The radiative lifetime τ_R of the emission state is

$$\tau_R=\frac{1}{A_T(aJ)}. \tag{15}$$

III. EXPERIMENTAL DETAILS

The rare-earth-doped lead borate glass samples were prepared using appropriate amounts of PbO of Analar quality, H_3BO_3 of Analar grade, and rare-earth oxides of high purity (99.9%) These raw materials were thoroughly mixed and melted in the range 800–1000 °C. The melt was air quenched by pouring it on a thick aluminum plate and covering it immediately with another aluminum plate. The samples were annealed at 300–350 °C for 5–6 h to remove thermal strains. All samples were characterized by x-ray technique and were found to be amorphous.

The systems studied are (a) 3 Nd_2O_3: 97 [xPbO:(100-x)B_2O_3] (BPN30-BPN70), (b) 3 Sm_2O_3: 97 [xPbO:(100-x)B_2O_3] (BPS30-BPS70), and (c) 1.5 Dy_2O_3: 98.5 [xPbO:(100-x)B_2O_3] (BPD30-BPD70) (x=30, 40, 50, 60, and 70 mol %). 3-mol % Dy_2O_3-doped lead borate glasses melt above 1000 °C, and because of the limitations of the furnace whose temperature cannot be raised beyond 1000 °C, we could not prepare samples with 3-mol % Dy_2O_3. However, with 1.5-mol % Dy_2O_3, the lead borate glasses melt below 1000 °C, and we could successfully prepare glasses doped with 1.5-mol % Dy_2O_3. The sample density is measured by the Archemedes method using xylene as the immersing liquid. The refractive index is measured by Bragg's reflection method using He-Ne laser as the source. Optical-absorption measurements were made using a Hitachi U3400 spectrophotometer, on optically polished glass samples of size 5×5×1 mm^3 (at room temperature) in the wavelength range 200–2400 nm (50 000–4166 cm^{-1}).

IV. RESULTS

A. Oscillator strengths

The absorption spectra of Nd^{3+}-, Sm^{3+}-, and Dy^{3+}-doped lead borates are shown in Figs. 2(a)–2(e). The oscillator strengths for different absorption bands of Nd^{3+}, Sm^{3+} (high- and low-energy region), and Dy^{3+} are determined using Eq. (3) and are given in Tables I–IV

For Sm^{3+}, the oscillator strengths are arranged into two groups,[11] one ''low-energy'' group corresponding to transitions up to 10 700 cm^{-1} and the other ''high-energy'' group corresponding to transitions in the energy range 17 600–32 800 cm^{-1}. The Ω_t parameters are calculated separately in the ''low-'' and ''high-'' energy regions. Since the Judd-Ofelt equation, Eq. (4), is applicable to cases where the high-f splittings are small as compared to the f-d energy gap, it is not appropriate to use the high-energy levels for the calculation of Ω_t. In Sm^{3+} the high-energy levels are close to the charge transfer band, and it is not appropriate to take these levels into calculation. It is seen that Ω_{2l} (low-energy region) is different from Ω_{2h} (high-energy region), indicating the different behavior of the low and high levels.

For Nd^{3+}, Sm^{3+}, and Dy^{3+} all the transitions are electric dipolar with significant intensities in the observed frequency range, except for the $^6H_{15/2}\rightarrow{}^6H_{13/2}$ transition (3500 cm^{-1}) of Dy^{3+}, which has a very small magnetic dipolar contribution[29] also. However, its overall intensity is very small and, therefore, is not taken into consideration while calculating the intensity parameters.

B. Intensity parameters

The best set of intensity parameters Ω_t (t=2,4,6) (for a given rare-earth ion) is obtained from the experimental oscillator strengths and the calculated doubly reduced matrix elements, using the expression for oscillator strength Eq. (10) by least-squares analysis. The intensity parameters determined for Nd^{3+}, Sm^{3+}, and Dy^{3+} for all the concentra-

TABLE II. Same as Table I, but for Sm^{3+} (3 mol %) the low-energy region.

Transitions from the ground state $^6H_{5/2}$	λ (nm)	Oscillator strength ($f\times10^{-8}$)									
		BPS30		BPS40		BPS50		BPS60		BPS70	
		f_{meas}	f_{cal}	f_{meas}	f_{cal}	f_{meas}	f_{cal}	f_{meas}	f_{cal}	f_{meas}	f_{cal}
$^6F_{1/2}$ (HST)	1514	58.2	56.8	39.4	37.3	47.9	45.7	50.0	47.5	41.8	39.7
$^6F_{3/2}$	1468	120.6	122.9	105.9	108.7	112.9	116.0	112.2	115.6	112.8	115.7
$^6F_{5/2}$	1365	191.2	189.2	187.6	187.1	191.6	190.7	187.2	186.9	199.5	199.2
$^6F_{7/2}$	1221	270.1	272.2	284.7	283.0	303.2	302.0	310.1	307.3	336.1	334.1
$^6F_{9/2}$	1072	173.0	171.4	178.7	180.6	194.9	196.9	200.7	203.3	220.3	221.9
$^6F_{11/2}$	938	32.1	27.9	30.2	29.4	36.2	32.3	30.7	33.5	32.9	36.6
RMS deviation		1.517%		1.098%		1.402%		1.460%		1.442%	
Density (g/cm^3)		4.302 ± 0.031		4.784 ± 0.030		5.265 ± 0.030		5.723 ± 0.020		6.053 ± 0.022	
N (10^{20} cm^{-3})		12.33 ± 0.087		12.22 ± 0.076		12.13 ± 0.069		12.01 ± 0.044		11.66 ± 0.044	
Refractive index		1.664 ± 0.01		1.711 ± 0.01		1.809 ± 0.01		1.835 ± 0.01		1.923 ± 0.01	
$\Omega_2\times10^{-20}$ cm^2		2.961 ± 0.203		1.878 ± 0.114		2.126 ± 0.110		2.164 ± 0.112		1.683 ± 0.089	
$\Omega_4\times10^{-20}$ cm^2		5.733 ± 0.251		5.575 ± 0.230		5.212 ± 0.191		4.999 ± 0.158		5.011 ± 0.189	
$\Omega_6\times10^{-20}$ cm^2		3.247 ± 0.193		3.312 ± 0.190		3.361 ± 0.183		3.418 ± 0.175		3.474 ± 0.198	

tions of PbO are listed in Tables I–IV. The experimental errors associated with the rare-earth ion concentration, refractive index, and sample thickness are taken into account. In order to estimate the accuracy of the intensity parameters obtained by the fitting, the root-mean-square deviations (δ_{RMS}) are calculated; δ_{RMS} is given by

$$\delta_{RMS}=\left[\frac{\Sigma(f_{cal}-f_{meas})^2}{\Sigma f_{meas}^2}\right]^{1/2}, \tag{16}$$

where f_{cal} and f_{meas} are the calculated and measured oscillator strengths, respectively, and the summation is taken over all the bands used to calculate the Ω_t parameters.

The intensity parameter Ω_2 for Nd^{3+} in lead borate glasses is found to decrease from 3.958×10^{-20} cm^2 to 3.588×10^{-20} cm^2 with an increase in PbO content from 30 to 40 mol %, as shown in Fig. 3(a). Ω_2 reaches a minimum around (45–50)-mol % PbO. With the further addition of PbO, Ω_2 increases slightly to 3.613×10^{-20} cm^2 and then decreases beyond 60-mol % PbO to 3.523×10^{-20} cm^2. For Sm^{3+}, the Ω_2 decreases markedly from 2.961×10^{-20} cm^2 to 1.878×10^{-20} cm^2 with an increase in the PbO content and reaches a minimum at (45–50)-mol % PbO [Fig. 3(b)]. Beyond 50 mol %, Ω_2 increases to 2.164×10^{-20} cm^2, and beyond 60 mol % it decreases to 1.683×10^{-20} cm^2. The Ω_2 parameter for Dy^{3+} initially decreases from 3.734×10^{-20} cm^2 to 3.498×10^{-20} cm^2, reaching a minimum around 40-mol % PbO, but it increases significantly beyond 40-mol % PbO [Fig. 3(c)].

The intensity parameter Ω_4 for all the ions decreases with an increase in PbO content [Figs. 4(a)–4(c)]. For Nd^{3+} and Sm^{3+}, Ω_6 increases from 4.882×10^{-20} cm^2 to 5.480×10^{-20} cm^2 and 3.247×10^{-20} cm^2 to 3.474×10^{-20} cm^2 with an increase in PbO content with a slope change at 45–50 mol % [Figs. 5(a) and 5(b)]. For Dy^{3+}, Ω_6 shows a minimum at 40-mol % PbO.

C. Hypersensitive transitions

The position and intensity of certain electric dipole transitions of rare-earth ions are found to be very sensitive to the environment of the rare-earth ion. Such transitions are termed as hypersensitive transitions by Jorgensen and Judd.[30] The hypersensitivity of a transition has been shown to be proportional to the nephlauxetic ratio β, which indicates the covalency of the R—O bond.[22] In the present work, the positions of the peak wavelengths of the hypersensitive bands (HST) of Nd^{3+} ($^4I_{9/2}\rightarrow{}^4G_{5/2},{}^2G_{7/2}$; 581 nm), Sm^{3+} ($^6H_{5/2}\rightarrow{}^6F_{1/2}$, 1512 nm), and Dy^{3+} ($^6H_{15/2}\rightarrow{}^6F_{11/2}$; 1262 nm) are investigated as a function of glass composition to study the nature of the R—O bond. For Nd^{3+} the peak wavelength shifts towards longer wavelengths from 581 to 583.9 nm and for Sm^{3+} from 1512.5 to 1518.7 nm. There is a slope change at 40-mol % PbO. For Dy^{3+}, the peak wavelength

TABLE III. Same as Table I, but for the high-energy region.

Sample	η	N (10^{20} cm^{-3})	ρ (g/cm^3)	Ω_2 (10^{-20} cm^2)	Ω_4 (10^{-20} cm^2)	Ω_6 (10^{-20} cm^2)
BPS30	1.664	12.326	4.302	80.435	17.12	6.600
BPS40	1.711	12.218	4.784	75.741	18.169	6.656
BPS50	1.809	12.132	5.265	67.96	18.463	6.753
PBS60	1.835	12.008	5.723	60.414	18.802	6.861
BPS70	1.923	11.662	6.053	52.927	18.997	6.945

TABLE IV. Same as Table I, but for Dy^{3+} (1.5 mol %).

Transitions from the ground state $^6H_{15/2}$	λ (nm)	Oscillator strength ($f\times10^{-8}$)									
		BPD30		BPD40		BPD50		BPD60		BPD70	
		f_{meas}	f_{cal}	f_{meas}	f_{cal}	f_{meas}	f_{cal}	f_{meas}	f_{cal}	f_{meas}	f_{cal}
$^6H_{11/2}$	1672	90.9	94.1	83.1	86.9	99.9	101.3	106.4	107.4	117.7	120.4
$^6F_{11/2},^6H_{9/2}$ (HST)	1263	431.4	431.2	408	407.8	458	457.9	473.4	473.3	504	503.9
$^6F_{9/2},^6H_{7/2}$	1085	200.1	199.5	179.4	179.3	212	211.3	213.5	212.9	205.5	205.8
$^6F_{7/2},^6H_{5/2}$	892	164.5	167.2	150.1	151.1	176.9	179.2	185.1	186.5	201.2	200.3
$^6F_{5/2}$	798	84.3	79.2	75.9	71.9	88.2	85.3	93.0	90.3	103.3	101.5
$^6F_{3/2}$	749	13.7	14.9	11.6	13.5	13.0	16.1	11.8	17.1	13.6	19.1
$^4F_{9/2}$	470	14.8	12.8	12.4	11.4	18.9	13.7	12.2	14.4	12.2	15.5
$^4I_{15/2}$	451	36.9	32.8	33.2	30.1	40.1	35.2	41.3	37.4	44.6	42.3
RMS deviation		1.705%		1.441%		1.584%		1.338%		1.236%	
Density (g/cm^3)		4.146±0.022		4.655±0.011		5.416±0.030		5.794±0.036		6.062±0.038	
N (10^{20} cm^{-3})		6.168±0.032		6.152±0.015		6.440±0.030		6.250±0.039		5.990±0.033	
Refractive index		1.652±0.01		1.700±0.01		1.743±0.01		1.804±0.01		1.906±0.01	
$\Omega_2\times10^{-20}$ cm^2		3.734±0.192		3.498±0.174		3.715±0.252		3.800±0.222		4.072±0.237	
$\Omega_4\times10^{-20}$ cm^2		1.320±0.059		1.120±0.066		1.265±0.041		1.087±0.064		0.616±0.046	
$\Omega_6\times10^{-20}$ cm^2		1.797±0.098		1.568±0.083		1.798±0.116		1.816±0.103		1.878±0.106	

varies from 1262.3 to 1267.1 nm [Figs. 6(a)–6(c)], and the variation of peak wavelength with composition shows a minimum at 40-mol % PbO.

The intensity (oscillator strength) of hypersensitive transitions shows a minimum value around 50-mol % PbO for Nd^{3+} and around (40–45)-mol % PbO for Sm^{3+} and Dy^{3+} (Tables I–IV) indicating a low asymmetry of the crystal field at the rare earth site at these compositions [Figs. 7(a)–7(c)].

To monitor the covalency of the Nd—O bond in the glass matrix, the variation of the spectral profiles of the transitions $^4I_{9/2}\rightarrow{}^4G_{5/2},{}^2G_{7/2}$ (HST) and $^4I_{9/2}\rightarrow{}^4F_{7/2},{}^4S_{3/2}$ of Nd^{3+} with a glass composition is also investigated. In these transitions, two peaks are distinguished by the Stark splitting and the relative intensity ratio between the peaks varied with the glass composition. The peak intensities of the short and long components are designated as I_S and I_L, respectively. An increase in the intensity ratio I_L/I_S is found to indicate a shift of the center of gravity of the absorption spectra to longer wavelengths.[31] This indicates an increase in the covalency of the Nd—O bond. Krupke[32] has pointed out that the transition intensities of $^4I_{9/2}\rightarrow{}^4G_{5/2},{}^2G_{7/2}$ and $^4I_{9/2}\rightarrow{}^4F_{7/2},{}^4S_{3/2}$ are determined mainly by the $\Omega_2|\langle\|U^{(2)}\|\rangle|^2$ and $\Omega_6|\langle\|U^{(6)}\|\rangle|^2$

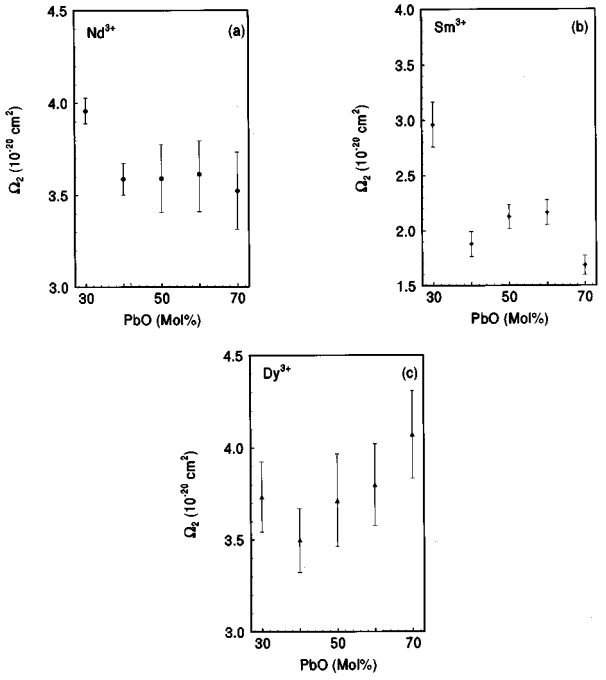

FIG. 3. Compositional dependence of Ω_2 parameters of (a) Nd^{3+}, (b) Sm^{3+}, and (c) Dy^{3+} in (100-x)B_2O_3:xPbO glasses.

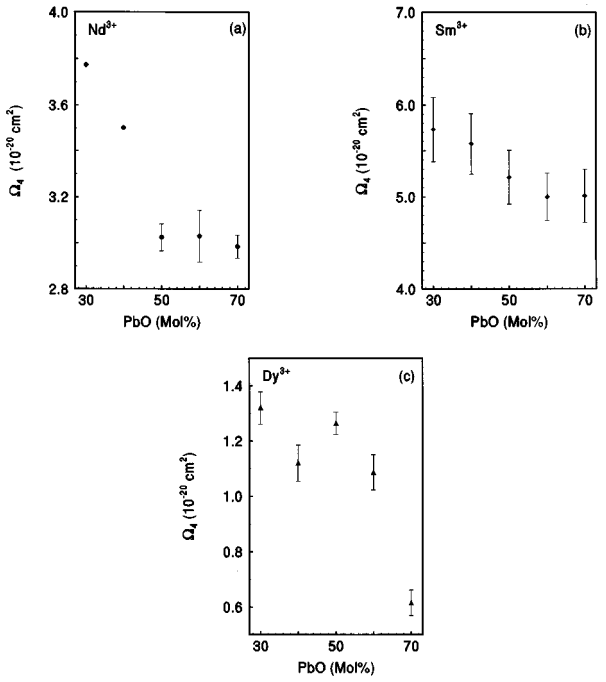

FIG. 4. Compositional dependence of Ω_4 parameters of (a) Nd^{3+}, (b) Sm^{3+}, and (c) Dy^{3+} in (100-x)B_2O_3:xPbO glasses.

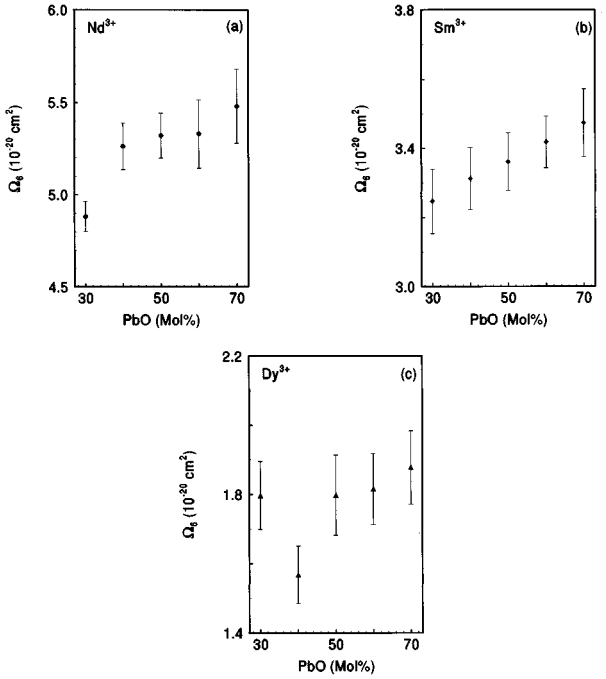

FIG. 5. Compositional dependence of Ω_6 parameters of (a) Nd^{3+}, (b) Sm^{3+}, and (c) Dy^{3+} in (100-x)B_2O_3:xPbO glasses.

terms, respectively. Therefore, from the relationship between the intensity parameters and relative intensity ratio I_L/I_S in these transitions, the effect of the Nd—O bond on the intensity parameters can be obtained.

In lead borate glasses, the Stark splitting of the transition $^4I_{9/2}\rightarrow{}^4G_{5/2},{}^2G_{7/2}$ is not well resolved. Hence, the dependence of Ω_2 on the intensity ratio I_L/I_S is not clear. Figure 8

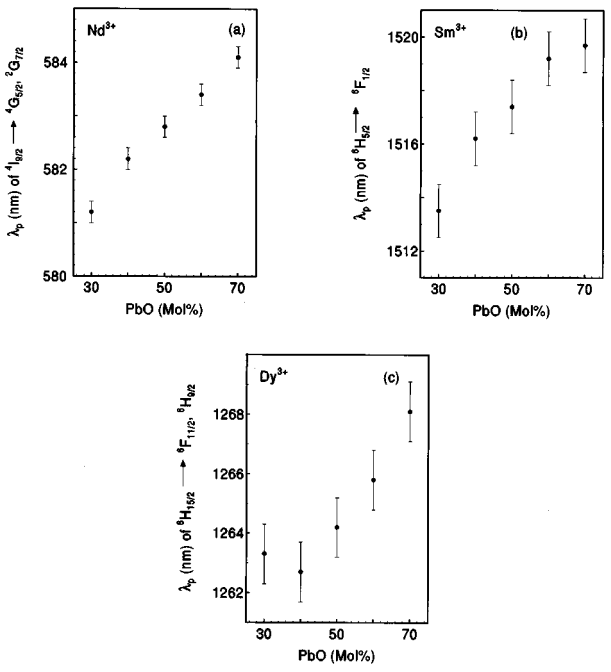

FIG. 6. Variation of peak wavelength λ_p of hypersensitive bands of (a) Nd^{3+}, (b) Sm^{3+}, and (c) Dy^{3+} in (100-x)B_2O_3:xPbO glasses.

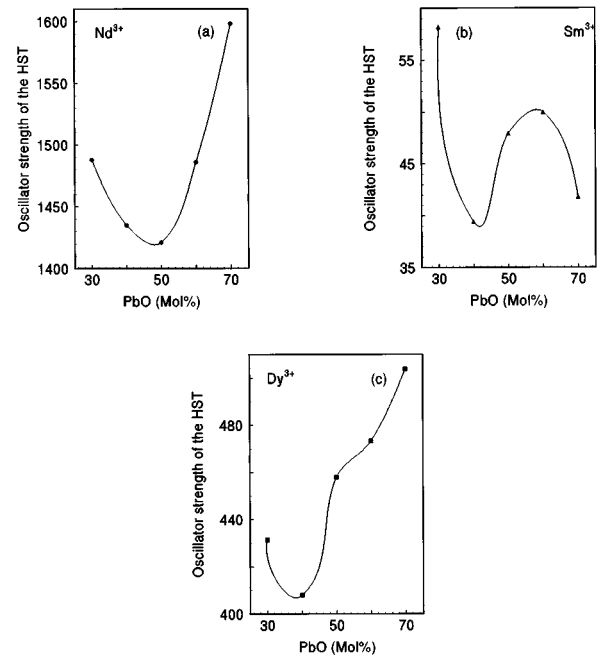

FIG. 7. Compositional dependence of the oscillator strength of the hypersensitive transitions of (a) Nd^{3+} ($^4I_{9/2}\rightarrow{}^4G_{5/2},{}^2G_{7/2}$), (b) Sm^{3+} ($^6H_{5/2}\rightarrow{}^6F_{1/2}$), and (c) Dy^{3+} ($^6H_{15/2}\rightarrow{}^6F_{11/2}$) in (100-$x$)$B_2O_3$:$x$PbO glasses.

shows the spectral profile of the transition $^4I_{9/2}\rightarrow{}^4F_{7/2},{}^4S_{3/2}$ of Nd^{3+} for different PbO concentrations. The relationship between the intensity parameter Ω_6 and the intensity ratio I_L/I_S (I_S=742 nm and I_L=749 nm) is shown in Fig. 9. The

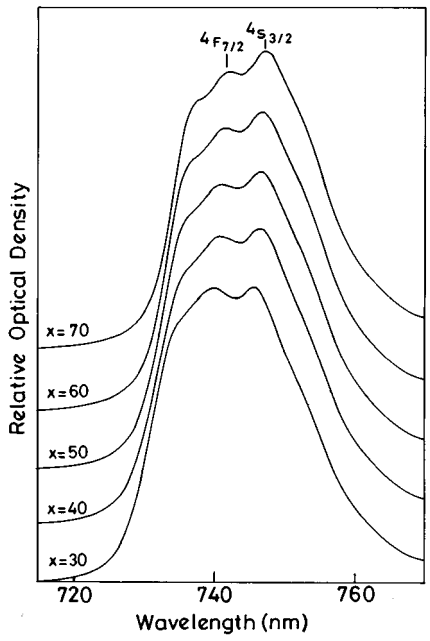

FIG. 8. Variation of spectral profile of the transition $^4I_{9/2}\rightarrow{}^4F_{7/2},{}^4S_{3/2}$ of Nd^{3+} with PbO content in (100-x)B_2O_3:xPbO glasses.

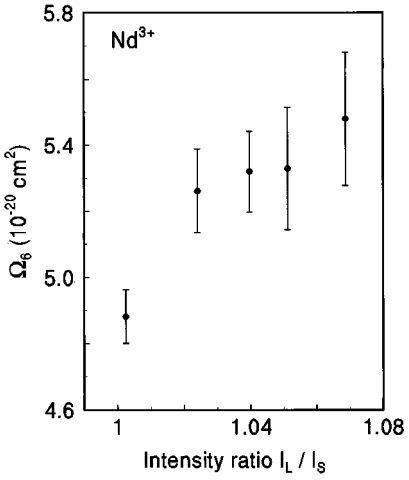

FIG. 9. Variation of Ω_6 with intensity ratio I_L/I_S of the transition $^4I_{9/2}\rightarrow{}^4F_{7/2},{}^4S_{3/2}$ of Nd^{3+} in $(100\text{-}x)B_2O_3$:xPbO glasses.

intensity parameter Ω_6 increases with increase in intensity ratio I_L/I_S, indicating an increase in covalency of Nd—O bond.

D. Radiative transition probability and branching ratios

Using Ω_t parameters, the radiative transition probability A_{rad} for spontaneous emission, radiative lifetime of the excited state from where fluorescence is observed, and branching ratios of Nd^{3+}, Sm^{3+}, and Dy^{3+} are calculated and presented in Tables V–VII for the $^4F_{3/2}$, $^4G_{5/2}$, and $^4F_{9/2}$ levels, respectively. A_{rad}, which depends on the intensity parameters and the refractive index n of the host material via the local field correction, is found to increase with PbO content, with a slope change around (45–50)-mol % PbO for all the three ions [Figs. 10(a)–10(c)].

V. DISCUSSION

A. Hypersensitive transitions and the R—O covalency

In lead borate glasses, the shift of the peak wavelengths of the hypersensitive bands of Nd^{3+} (580 nm), Sm^{3+} (1512 nm), and Dy^{3+} (1262 nm) towards longer wavelengths with an increase in PbO content [Figs. 2(a)–2(e)], because of nephlauxetic effect,[33] indicates that the degree of covalency of the R—O bond increases with PbO content. This is because of the tightening of the structure with the formation of BO_4 units and PbO_4 units, which results in increased interaction between the rare-earth ion and the charged nonbridging oxygen atoms (NBO's). NBO's are formed after 35-mol % PbO and increase with PbO content.[17] A similar shift of the peak wavelength of the hypersensitive transition of Nd^{3+} to longer wavelengths has been reported in halide complexes [NdI_3 (g), $NdBr_3$ (g), NdI_3 (l), NdI_3 (s), and Nd (ethylene diamine tetra acetic acid)$^-$] by Henrie and Choppin.[31] The degree of covalency of the Nd—O bond in these complexes increases in the order Cl<Br<I.

The dependence of the intensity parameter Ω_2 on the intensity ratio I_L/I_S of the transition $^4I_{9/2}\rightarrow{}^4G_{5/2},{}^2G_{7/2}$ could not be ascertained because of the poor resolution of the crystal-field split levels, whereas Ω_6 is found to increase with I_L/I_S of the transition $^4I_{9/2}\rightarrow{}^4F_{7/2},{}^4S_{3/2}$. An increase in I_L/I_S indicates an increase in the covalency of the Nd—O bond. Thus Ω_6 is an indicator of the covalency of the R—O bond. Similar behavior for Ω_6 is observed in Nd^{3+}-doped alkali silicate and alkali borate glasses also.[2]

B. Intensity parameters

1. Variation of Ω_t parameters of Nd^{3+} and Sm^{3+} in lead borate glasses

In lead borate glasses, the covalency of R—O bond increases with an increase in PbO content as indicated by the shift of the hypersensitive bands towards longer wavelengths and the increase in the intensity ratio of the transition $^4I_{9/2}\rightarrow{}^4F_{7/2},{}^4S_{3/2}$ with PbO content. This implies that $\Xi(s,t)$ increases with PbO content. The intensity parameter Ω_2 for Nd^{3+} and Sm^{3+} initially decreases with an increase in PbO content [Figs. 3(a) and 3(b)] and reaches a minimum around (45–50)-mol %, PbO, indicating that $A_{s,p}$ alone is responsible for the decrease of Ω_2. The addition of PbO to B_2O_3 converts three coordinated boron atoms (B_3) to four coordinated boron atoms (B_4) resulting in the conversion of boroxol units to pentaborate groups.[34] The fraction of B_4 in the form of diborate units is maximum around (45–50)-mol % PbO. At this composition the asymmetry of the ligand field at the rare-earth site is less. This is also indicated by the lower oscillator strengths of the hypersensitive transitions of Nd^{3+} and Sm^{3+} [Tables I and II]. It has been proposed[35] that in oxide glasses a rare-earth ion is surrounded by eight neighboring oxygen atoms belonging to the corners of BO_4, PbO_4, or any glass-forming tetrahedra (Fig. 11). Each tetrahedron donates two oxygen atoms, forming an edge of the

TABLE V. Radiative transition probability A_{rad}, radiative lifetime τ_R, and branching ratios β_R of Nd^{3+} in $(100\text{-}x)$ $B_2O_3$$x$PbO glasses.

Transitions from $^4F_{3/2}\rightarrow$	ν (cm^{-1})	BPN30		BPN40		BPN50		BPN60		BPN70	
		A (sec^{-1})	β_R	A (sec^{-1})	β_R	A (sec^{-1})	β_R	A (sec^{-1})	β_R	A (sec^{-1})	β_R
$^4I_{15/2}$	5450	17.0	0.005	20.0	0.005	22.0	0.006	24.0	0.006	31.0	0.006
$^4I_{13/2}$	7515	330	0.101	401	0.107	436	0.113	481	0.113	609	0.114
$^4I_{11/2}$	9515	1656	0.506	1953	0.520	2069	0.534	2279	0.534	2872	0.538
$^4I_{9/2}$	11 392	1270	0.388	1381	0.368	1344	0.347	1481	0.347	1825	0.342
ΣA (sec^{-1})		3273±35		3754±12		3871±58		4265±125		5336±219	
τ_R (μsec)		306±4		266±1		258±4		234±8		187±8	

TABLE VI. Same as Table V, but for Sm^{3+}.

Transitions from $^4G_{5/2}\rightarrow$	ν (cm^{-1})	BPS30		BPS40		BPS50		BPS60		BPS70	
		A (sec^{-1})	β_R	A (sec^{-1})	β_R	A (sec^{-1})	β_R	A (sec^{-1})	β_R	A (sec^{-1})	β_R
$^6F_{9/2}$	8700	2.2	0.004	1.8	0.003	2.3	0.004	2.4	0.004	2.4	0.003
$^6F_{7/2}$	9900	4.4	0.009	4.7	0.009	5.3	0.009	5.4	0.009	6.4	0.009
$^6F_{5/2}$	10 800	16.9	0.034	14.0	0.027	17.0	0.029	18.0	0.030	18.0	0.026
$^6F_{3/2}$	11 300	2.2	0.004	1.5	0.003	2.1	0.004	2.2	0.004	2.0	0.003
$^6H_{13/2}$	12 900	5.0	0.010	5.5	0.011	6.8	0.012	7.0	0.012	9.0	0.012
$^6H_{11/2}$	14 300	47.0	0.096	50.6	0.101	58.0	0.099	59.0	0.098	71.0	0.100
$^6H_{9/2}$	15 600	134	0.274	123	0.246	150	0.254	155	0.256	169	0.241
$^6H_{7/2}$	16 800	166	0.339	180	0.360	211	0.357	217	0.357	259	0.368
$^6H_{5/2}$	17 854	112	0.229	120	0.240	138	0.234	140	0.231	167	0.237
ΣA (sec^{-1})		489±20		502±20		590±21		608±20		703±28	
τ_R (μsec)		2043±92		1993±84		1694±65		1646±56		1423±58	

cube. This implies that around (45–50)-mol % PbO the symmetry of the crystal field is high at the rare-earth-ion site.

With the further addition of PbO up to 65 mol %, back conversion of B_4 to B_3 with the formation NBO's takes place, which leads to an increase in the distortion of the ligand field at the rare-earth site and covalency of the R—O bond. Hence, in this region both $\Xi(s,t)$ and $A_{s,p}$ are responsible for the increase of Ω_2. Beyond 65-mol % PbO, Ω_2 decreases, indicating a decrease in the asymmetry of the crystal field at the rare-earth site. In this region, the majority of the oxygen atoms are NBO's, leading to a more ordered environment around the rare-earth ion. On the other hand, Ω_6 increases with an increase in PbO content, indicating that $\Xi(s,t)$ is responsible for the increase. This implies that Ω_6 is an indicator of R-O covalency [Figs. 5(a) and 5(b)].

The magnitude of Ω_2 is small in lead borate glasses compared to other borates[2] and tellurites.[36] In lead borate glasses, the high polarizability of the Pb ions and the directional and covalent nature of the Pb—O bond induce a more symmetric crystal field on the rare-earth ions. This reduces the mixing of opposite parity electronic configurations, which are responsible for the spectral intensities.

The intensity parameter Ω_6, which is an indicator of the covalency of the R—O bond, is affected by two factors. (1) The addition of PbO to B_2O_3 converts B_3 to B_4. The increase in BO_4 units by the addition of PbO leads to the closer packing of oxygen atoms, which in turn increases the covalency of the R—O bond. (2) The nonbridging oxygen atoms (NBO's) are formed beyond 35-mol % PbO with the formation of metaborate groups. They persist until 70-mol % PbO. Since NBO's possess a negative charge, the electrostatic attraction between NBO's and rare-earth ions is strong, which leads to the attraction of NBO's closer to the rare-earth ion. This increases the overlapping of ligand orbitals and the $4f$ orbitals and, hence, the covalency.

2. Variation of Ω_t parameters of Dy^{3+} in lead borate glasses

The intensity parameter Ω_2 initially decreases [Fig. 3(c)] but increases beyond 40 mol %. This implies that Ω_2 is mainly dependent on $\Xi(s,t)$ rather than on $A_{s,p}$ beyond 40 mol %. As $4f$ electrons in the rare-earth atoms are well shielded by the outer $5s$ and $5p$ shells, the effective nuclear charge increases with increasing atomic number from Nd to Dy, causing a reduction in the size of the $4f$ shell and a decrease in atomic or ionic radius from Nd to Dy (1 to 0.91 Å). Consequently, the Dy-O distance is smaller than the Nd-O or Sm-O distances. This leads to an increase in the

TABLE VII. Same as Table V, but for Dy^{3+}.

Transitions from $^4F_{9/2}\rightarrow$	ν (cm^{-1})	BPD30		BPD40		BPD50		BPD60		BPD70	
		A (sec^{-1})	β_R	A (sec^{-1})	β_R	A (sec^{-1})	β_R	A (sec^{-1})	β_R	A (sec^{-1})	β_R
$^6H_{15/2}$	21 237	167	0.220	159	0.213	199	0.221	223	0.219	268	0.214
$^6H_{13/2}$	17 771	504	0.667	505	0.674	600	0.667	681	0.670	851	0.678
$^6H_{11/2}$	15 444	47	0.062	48	0.064	56	0.062	64	0.063	81	0.064
$^6H_{9/2}$	13 585	13	0.017	12	0.016	15	0.016	17	0.016	20	0.016
$^6H_{7/2}$	12 162	14	0.018	13	0.017	16	0.018	17	0.017	18	0.014
$^6H_{5/2}$	11 108	3	0.004	3	0.003	3	0.003	3	0.003	3	0.002
$^6F_{7/2}$	10 252	4	0.005	4	0.005	4	0.005	5	0.005	5	0.004
$^6H_{5/2}$	8 845	5	0.007	5	0.007	6	0.007	7	0.007	9	0.007
ΣA (sec^{-1})		755±30		749±25		899±40		1015±10		1254±50	
τ_R (μsec)		1324±45		1336±46		1112±52		985±40		797±34	

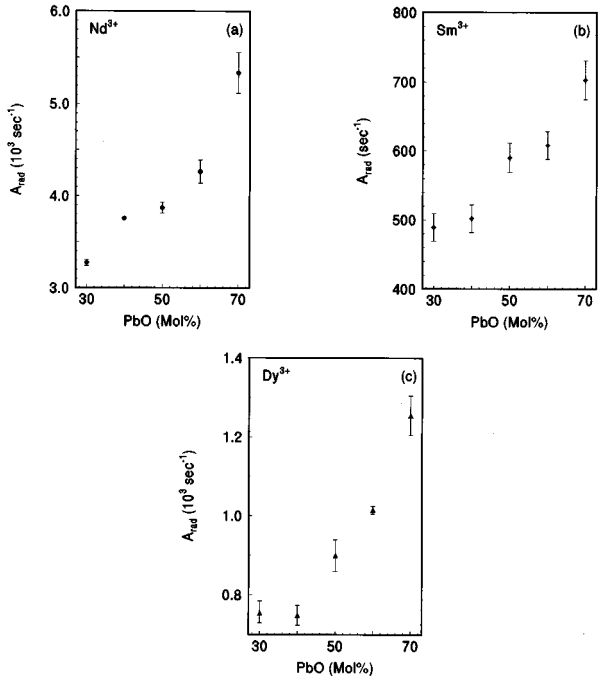

FIG. 10. Compositional dependence of A_{rad} of (a) Nd^{3+}, (b) Sm^{3+}, and (c) Dy^{3+} in $(100\text{-}x)B_2O_3$:xPbO glasses.

nephlauxetic effect, and an increase of Ω_2. Ω_6 shows a minimum at 40-mol % PbO and then increases [see Fig. 5(c)]. The reason for the minimum in the variation of Ω_6 with the PbO content is not immediately obvious.

Thus, in Nd^{3+}- and Sm^{3+}-doped lead borate glasses, both $A_{s,p}$ and $\Xi(s,t)$ play an important role in the variation of Ω_2 with PbO content, while in Dy^{3+}-doped glasses only $\Xi(s,t)$ is dominant in determining Ω_2. Ω_6 mainly depends on $\Xi(s,t)$ for all the three ions.

Generally, it is observed that in silicate and borate glasses,[2,6,7,37,38] Ω_2 is determined by the asymmetry of the ligand field at the rare-earth site and the nephlauxetic effect, while Ω_6 depends only on the nephlauxetic effect. On the other hand, in phosphate glasses all the three parameters depend strongly on the ionic radius of the modifier.[2]

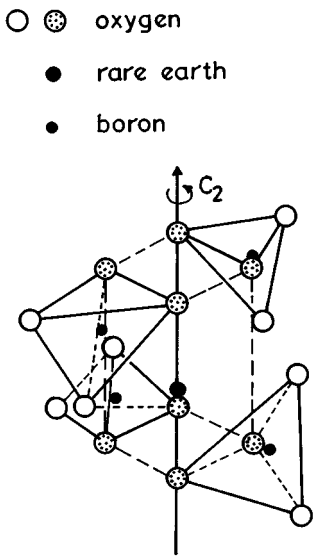

FIG. 11. Proposed rare-earth-site model (Ref. 35).

C. Radiative transition probability for electric dipole emission and branching ratios

The variation of A_{rad} with PbO content indicates an increasing order around the rare-earth ion at (45–50)-mol % PbO. The large radiative transition probability in lead borate glasses arises from the large refractive index of the host glass. The refractive index of the lead borate glasses increases with an increase in PbO content from $\approx$1.6 to $\approx$2 (see Tables I–III). The stimulated emission cross sections σ (Ref. 1) of the fluorescence lines of rare-earth ions can be calculated using A_{rad}. Because of the strong dependence of A_{rad} on the refractive index, σ could be quite high for the lasing transitions of the rare-earth ions in lead borate glasses.

The large stimulated emission cross sections are attractive features for low-threshold, high-gain applications and are utilized to obtain cw laser action. In tellurite glasses[36] doped with Nd^{3+} the radiative transition probabilities are large and, hence, so are the stimulated emission cross sections. Laser action has been observed in these systems. The radiative transition probabilities in lead borate glasses are of the order of those reported in tellurite glasses, and, hence, lead borate glass can be a potential laser host material. In lead borate glasses, large quantities of rare-earth ions can be doped and, therefore, can be utilized for high-concentration minilasers.

The branching ratios β_R are evaluated for each transition and probable lasing transitions of the rare-earth ions are as shown in Figs. 12(a)–12(c). The branching ratios of the lasing transitions are high compared to other transitions. (See Tables V–VII.)

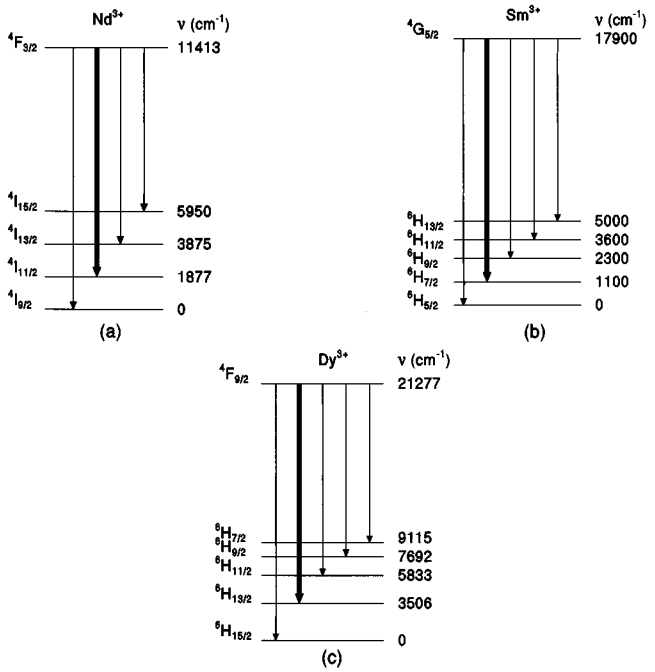

FIG. 12. Lasing transitions of (a) Nd^{3+} ($^4F_{3/2}\rightarrow{}^4I_{11/2}$), (b) Sm^{3+} ($^4G_{5/2}\rightarrow{}^6H_{7/2}$), and (c) Dy^{3+} ($^4F_{9/2}\rightarrow{}^6H_{13/2}$) in $(100\text{-}x)B_2O_3$:xPbO glasses.

VI. CONCLUSIONS

Using the Judd-Ofelt theory, the three intensity parameters, spontaneous emission probabilities, and radiative lifetimes of Nd^{3+}, Sm^{3+}, and Dy^{3+} ions doped in lead borate glasses are determined. The changes in the position and the intensity parameters of the transitions in the optical-absorption spectra of the ions are correlated to the structural changes in the host glass matrix. The shift of the hypersensitive bands of Nd^{3+} ($^4I_{9/2}\rightarrow{}^4G_{5/2},{}^2G_{7/2}$; 581 nm), Sm^{3+} ($^6H_{5/2}\rightarrow{}^6F_{1/2}$; 1512 nm), and Dy^{3+} ($^6H_{15/2}\rightarrow{}^6F_{11/2}$; 1262 nm) shows that the covalency of the *R*—O bond increases with an increase in PbO content, because of the increased interaction between rare-earth ions and nonbridging oxygen atoms. The variation of the spectral profile of the transition $^4I_{9/2}\rightarrow{}^4F_{7/2},{}^4S_{3/2}$ also indicates an increase in the covalency of the *R*—O bond.

The variation of the intensity parameter Ω_2 with PbO content for Nd^{3+} and Sm^{3+} implies that both asymmetry of the crystal field at the rare-earth site and nephlauxetic effect play an important role in determining the intensity, whereas in Dy^{3+}-doped glasses, nephlauxetic effect plays a dominant role.

The radiative emission probability for the Nd^{3+} ion is as high as in tellurite glasses, which have been used as laser host material. This indicates that the lead borate glasses may also be useful as laser materials.

ACKNOWLEDGMENTS

The authors gratefully acknowledge Professor Y. V. G. S. Murthy for extending the experimental facilities and for fruitful discussions.

[1] R. Reisfeld and C. K. Jorgensen., *Lasers and Excited States of Rare Earths* (Springer-Verlag, Berlin, 1977).
[2] Y. Nageno, H. Takebe, and K. Morinaga, J. Am. Ceram. Soc. **76**, 3081 (1993).
[3] T. Izumitani, H. Toratani, and H. Kuroda, J. Non-Cryst. Solids. **47**, 87 (1982).
[4] M. Zahir, R. Olazcuaga, C. Parent, G. Le Flem, and P. Hagnmuller, J. Non-Cryst. Solids. **69**, 221 (1985).
[5] R. Cases, M. A. Chamarro, R. Alcala, and V. D. Rodriguez, J. Lumin. **48&49**, 509 (1991).
[6] K. Gatterer, G. Pucker, H. P. Fritzer, and S. Arafa, J. Non-Cryst. Solids. **176**, 237 (1994).
[7] M. J. Weber, L. A. Boatner, and B. C. Sales, J. Non-Cryst. Solids. **74**, 167 (1985).
[8] J. L. Adam, A. D. Docq, and J. Lucas, J. Solid State Chem. **75**, 403 (1988).
[9] R. Reisfeld, A. Bornstein, and L. Boehm, J. Solid State Chem. **14**, 14 (1975).
[10] M. Canalejo, R. Cases, and R. Alcala, Phys. Chem. Glasses **29**, 187 (1988).
[11] L. Booehm, R. Reisfeld, and N. Spector, J. Solid State Chem. **28**, 75 (1979).
[12] R. Reisfeld, E. Greenberg, and E. Biron, J. Solid State Chem. **9**, 224 (1974).
[13] B. R. Judd, Phys. Rev. **127**, 750 (1962).
[14] G. S. Ofelt, J. Chem. Phys. **37**, 511 (1962).
[15] A. Paul, Phys. Chem. Glasses **11**, 46 (1970).
[16] P. J. Bray, M. Leventhal, and H. O. Hooper, Phys. Chem. Glasses **4**, 47 (1963).
[17] B. N. Meera, A. K. Sood, N. Chandrabhas, and J. Ramakrishna, J. Non-Cryst. Solids **126**, 224 (1990).
[18] W. T. Carnall, P. R. Fields, and B. G. Wybourne, J. Chem. Phys. **42**, 3797 (1963).
[19] C. K. Jorgensen, *Absorption Spectra and Chemical Bonding in Complexes* (Pergamon, New York, 1962).
[20] R. D. Peacock, in *Structure and Bonding*, edited by J. D. Dunitz *et al.* (Springer-Verlag, Berlin, 1975), Vol. 22.
[21] R. Reisfeld, in *Structure and Bonding*, edited by J. D. Dunitz *et al.* (Springer-Verlag, Berlin, 1975), Vol. 22.
[22] C. K. Jorgensen, *Modern Aspects of Ligand Field Theory* (North-Holland, Amsterdam, 1971).
[23] B. R. Judd, Proc. Phys. Soc. London, Ser. A **69**, 157 (1956).
[24] M. J. Weber, Phys. Rev. **157**, 262 (1967).
[25] W. T. Carnall, P. R. Fields, and K. Rajnak, J. Chem. Phys. **49**, 4443 (1968).
[26] C. W. Neilson and G. F. Koster, *Spectroscopic Coefficients for the p, d, and f Configurations* (MIT Press, Cambridge, Massachusetts, 1964).
[27] D. C. Yeh, W. A. Sibley, M. Suscavage, and M. G. Drexage, J. Non-Cryst. Solids **88**, 66 (1986).
[28] D. C. Brown, *High Peak Power Nd: Glass Laser Systems* (Springer-Verlag, Berlin, 1981).
[29] M. D. Shinn, W. A. Sibley, M. G. Drexage, and R. N. Brown, Phys. Rev. B. **27**, 6635 (1983).
[30] C. K. Jorgensen and B. R. Judd, Mol. Phys. **8**, 281 (1964).
[31] D. E. Henrie and G. R. Choppin, J. Chem. Phys. **49**, 477 (1968).
[32] W. F. Krupke, IEEE J. Quantum Electron. **QE-10**, 450 (1974).
[33] C. K. Jorgensen, Prog. Inorg. Chem. **4**, 73 (1962).
[34] B. N. Meera, Ph.D. thesis, Indian Institute of Science, 1992.
[35] R. Reisfeld and Y. Eckstein, J. Solid State Chem. **5**, 174 (1972).
[36] M. J. Weber, J. D. Myers, and D. H. Blackburn, J. Appl. Phys. **52**, 2944 (1981).
[37] M. J. Weber, R. A. Saroyan, and R. C. Ropp, J. Non-Cryst. Solids **44**, 137 (1981).
[38] S. Tanabe, T. Ohayagi, N. Soga, and T. Hanada, Phys. Rev. B **46**, 3305 (1992).